Physics – Uspekhi **64** (5) 452 – 467 (2021)

REVIEWS OF TOPICAL PROBLEMS PACS numbers: 94.20.ws, **94.30. – d**, 94.30.Ms

Frequency-modulated ultra-low-frequency waves in near-Earth space

A V Guglielmi, A S Potapov

DOI: https://doi.org/10.3367/UFNe.2020.06.038777

Contents

Abstract. This review is devoted to ultra-low-frequency electromagnetic waves of a natural origin. A variety of frequency-modulated waves whose sources are located in the ionosphere, in the radiation belt, on the periphery of the magnetosphere, and in the solar wind in front of the magnetosphere bow shock are considered. The main focus is on the mechanisms of the formation of frequency modulation. Analysis of frequency modulation gives us information about the processes of excitation and propagation of waves, as well as about physical conditions in places of excitation and along signal propagation paths. Relevant open question about the physics of frequency-modulated waves are indicated.

Keywords: plasma, solar wind, magnetosphere, radiation belt, electromagnetic waves, ion cyclotron instability, dispersion, Doppler effect

1. Introduction

The near-earth space extends from the lower ionosphere (altitude of about 90 km) to the boundary of the magnetosphere. The magnetosphere, strongly elongated in the anti-solar direction, is bounded by the so-called magnetopause, the distance to which in the direction of the Sun is about 70,000 km [1]. A rich variety of frequency-modulated electromagnetic waves is excited and propagates in these vast expanses. We focus our attention on waves in the range of ultra-low frequencies (ULFs) — from several millihertz to several hertz [2]. A distinguishing feature of ULF waves is that their properties are essentially dependent on the ion component of space plasma [3].

The classification of ULF electromagnetic pulsations was developed by scientists at the Borok Observatory of the Institute of Physics of the Earth, led by V A Troitskaya, at the beginning of the 1960s (see, e.g., Refs [2–4]). The classification is based on a morphological principle and uses a binary name convention. All pulsations are split into two classes abbreviated as Pc (*pulsations continuous*) and Pi (*pulsations irregular*). The types of pulsations are denoted by the symbols Pc1 (0.2–5 s), Pc2 (5–10 s), Pc3 (10–45 s), Pc4 (45–150 s), Pc5 (150–600 s), Pi1 (1–40 s), and Pi2 (40–150 s). For reference, the related ranges of pulsation periods are given in parentheses. This classification was approved by the Thirteenth General Assembly of the International Union of Geodesy and Geophysics in Berkeley in August 1963. It is still widely used in the geophysical literature, giving the opportunity to become oriented in the rich variety of ULF pulsations of terrestrial and space origin.

Special names are usually given to the some varieties of pulsations. For example, Pc1 waves with the dynamical spectrum shown in Fig. 1 are commonly referred to as *pearl necklaces*. A general view on the origin of the pearls is that these pulsations are generated in the outer radiation belt and propagate to Earth along geomagnetic field lines. The event shown in Fig. 1 was observed before midnight local time. The signal was recorded from the exit of an LEMI-30 inductive magnetometer at the Norilsk high-latitude Integrated Magnetic-Ionospheric Station at a low level of geomagnetic activity. The series of pulsations consists of a quasi-periodic

A V Guglielmi [1, a], **A S Potapov** [2, b]
[1] Schmidt Institute of Physics of the Earth,
Russian Academy of Sciences,
ul. Bol'shaya Gruzinskaya 10, str. 1, 123242 Moscow,
Russian Federation
[2] Institute of Solar-Terrestrial Physics,
Siberian Branch of the Russian Academy of Sciences,
ul. Lermontova 126A, 664033 Irkutsk, Russian Federation
E-mail: [a] guglielmi@mail.ru, [b] potapov@iszf.irk.ru

Received 29 March 2020, revised 9 June 2020
Uspekhi Fizicheskikh Nauk **191** (5) 475 – 491 (2021)
Translated by S D Danilov

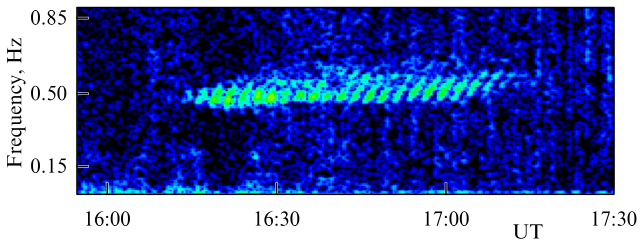

Figure 1. (Color online.) Variety of Pc1 waves known as pearls. The waves were recorded at the Norilsk Observatory on 03.05.2012. UT is universal time.

sequence of structural elements. For brevity, they are sometimes called *risings* or signals of ascending tone. In Fig. 1, the risings are repeated every 160 s on average. The length of the series is about 1 h; its carrier frequency stays nearly constant in time, increasing slightly from 0.50 Hz at the beginning of the series to 0.56 Hz at its end.

The analysis of frequency modulation gives us information on the mechanisms of wave excitation and propagation, and also on physical conditions at the locations the waves were excited and on the paths they traveled. It is quite clear that in natural conditions the frequency modulation is accompanied by amplitude modulation. However, first, the amplitude modulation is less informative than the frequency modulation, and second, it is already thoroughly explored and described in the available review literature. Namely this motivated the choice of the topic of the present review. In writing it, we tried to account for the valuable experience of the domestic radiophysics school gained in work on the theory of modulated pulsations and waves [5, 6]. It is worth noting that this experience also includes the development of the theory of whistling atmospherics which are excited in the radio range in lightning discharges and propagate along long paths in near-earth space [7, 8].

The experimental and theoretical study of ULF waves is the subject of a vast literature (see, for example, reviews and monographs [2–4, 8–15] and references therein). However, earlier, no special attention was paid to the frequency modulation which is particularly prominent in the upper part of the ULF range. We are trying to fill this gap in this review. In Sections 2–5, we consider a variety of frequency modulated waves with sources located in the solar wind, at the periphery of the magnetosphere, and in the radiation belt. We will present waves typical of quiet conditions, as well as waves that occur sporadically during magnetic storms. We are interested, first of all, in the mechanisms of frequency modulation, with Section 3 being devoted to one of the most complicated problems in the physics of the magnetosphere — the problem of the pearl origin. Section 6 deals with questions that were not touched on in the preceding sections. The final section proposes a summary and points to unsolved problems that are promising for further research.

2. Serpentine emission

2.1 Cyclotron instability of interplanetary plasma

With rare exceptions, ULF waves are self-excited because of the instability of nonequilibrium space plasma. A nonequilibrium state is typical of the magnetospheric plasma, but we will start from afar and consider first and foremost the self-excitation of ULF waves in the interplanetary plasma, which is also off equilibrium and is unstable by virtue of the factors that give birth to the solar wind. The solar wind speed is much higher than the speed of ULF waves. As a result, waves that are excited in the interplanetary space in front of the magnetospheric bow shock are carried by the solar wind on the magnetosphere and can be detected inside the magnetosphere and on Earth's surface.

According to our understanding [16–19], *serpentine emission* (SE), which will be discussed below, occurs precisely in this way. SE represents a variety of Pc1–2 waves characterized by deep deviations in the carrier frequency. The SE carrier frequency is governed by processes in the interplanetary space, and the modulating factor is governed by even more remote processes — on the Sun, where it appears spontaneously in chromospheric flares or is permanently available in the form of helioseismic oscillations of the photosphere.

The mechanism of SE excitation is seen by us as follows. According to Parker [20], an adiabatic expansion of the solar corona, which is detected by spacecraft as the solar wind, is on its own a permanently acting factor that forms anisotropy in pressure in the interplanetary plasma. The field lines of the interplanetary magnetic field (IMF) twisted in the Parker spirals because of the Sun's rotation serve as the axis of anisotropy. A theory predicts that in Earth's orbit the longitudinal proton temperature $T_\parallel$ is approximately twice as high as the transverse temperature $T_\perp$. For such a ratio between the temperatures, a short-wave ion-cyclotron instability develops in a hot interplanetary plasma, which can be the reason behind SE excitation [21].

Generally speaking, magnetic hydrodynamics predicts that in hot plasmas a long-wave hose instability may develop for a sufficiently large ratio $T_\parallel/T_\perp$. At one time, it was suggested that the hose instability lowers the theoretically admissible value $T_\parallel/T_\perp = 2$ to values $T_\parallel/T_\perp \approx 1.2$, as actually measured by spacecraft [22]. Yet, most likely, it is the kinetic cyclotron instability that leads to the reduction in anisotropy, and not the hydrodynamical hose instability. Furthermore, the hose instability can be suppressed altogether in an expanding solar corona [23], similarly to the suppression of the Jeans gravitational instability in an expanding Universe [24].

As shown in Ref. [21], in a reference frame co-moving with the speed of the solar wind, the frequency of ion-cyclotron waves ω' is on the order of proton gyrofrequency $\Omega_\mathrm{p} = eB/(m_\mathrm{p}c)$, and the instability increment is approximately expressed as

$$\gamma(k_\parallel, \theta) = \mu(k_* - k_\parallel) \exp\left[-\left(\frac{k_0}{k_\parallel}\right)^2\right] - \eta\theta^2 . \qquad (1)$$

Here, $k_\parallel = |k_z|$ in the Cartesian reference frame with the z-axis directed along the vector **B** of the IMF, **k** is the wave vector, θ is the angle between the vectors **B** and **k**, $\theta^2 \ll 1$ (paraxial approximation), e and m_p are the proton charge and mass, and c is the speed of light. We conclude that the increment depends on four parameters: μ, k_*, k_0, and η. We refrain from presenting the relationship between these parameters on one side and the parameters of interplanetary plasma on the other side, because they are rather unwieldy. For us, it is only important that, in a typical case, $k_* > 0$, $\eta > 0$, $\mu > 0$ and that the increment $\gamma(k_\parallel, \theta)$ reaches its maximum at $\theta = 0$ and $k_\parallel = k_\mathrm{m} \sim \omega_{0\mathrm{p}}/c$, $\omega_{0\mathrm{p}} = \sqrt{4\pi e^2 N/m_\mathrm{p}}$, where N is the proton concentration [21].

Now, we take into account small perturbations of the concentration N which are present in real plasma. Scattering on small-scale density fluctuations leads to broadening of the wave angular spectrum. Let us assume that waves are scattered over small angles. We also suppose that the mean angle of scattering equals zero and denote the mean square value of the scattering angle by $\langle\theta^2\rangle$. Now, we average $\gamma(k_\parallel, \theta)$ over θ and denote the result of averaging as $\gamma(k_\parallel)$. The value of $\gamma(k_\parallel)$ is defined by the right-hand side of Eqn (1), where θ^2 is replaced by the quantity $\langle\theta^2\rangle$. We expand the function $\gamma(k_\parallel)$ in the vicinity of its maximum,

$$\gamma(k_\parallel) = \gamma_\mathrm{m}\left[1 - \frac{(k_\parallel - k_\mathrm{m})^2}{\Delta k^2}\right]. \tag{2}$$

The maximum of increment γ_m and the width of instability interval Δk are defined by the parameters μ, η, k_*, k_0, and $\langle\theta^2\rangle$. We will not discuss them in detail, since we are interested only in the general structure of Eqn (2).

Qualitatively, the evolution of small perturbations looks like the following. Small perturbations grow through their linear stage, their angular range rapidly narrows, and their wave numbers become concentrated in a small vicinity of k_m. Nonlinear processes gradually enter the game as the amplitude grows, which leads to the modulation instability of the wave field. The result is the broadening of the spectrum. It leads to energy transfer from the amplification region ($|k_\parallel - k_\mathrm{m}| < \Delta k$) to the region of dissipation ($|k_\parallel - k_\mathrm{m}| > \Delta k$). The wave energy becomes stabilized, being redistributed over the spectrum.

2.2 Doppler mechanism of frequency modulation

Thus, the anisotropy of interplanetary plasma leads to the self-excitation of waves whose fronts are orthogonal to the IMF. In a co-moving frame of reference, the wave frequency is of the order of $\omega' \sim \Omega_\mathrm{p}$ at $k_\parallel = k_\mathrm{m}$. In the laboratory reference frame (on Earth or in a spacecraft), the frequency

$$\omega = \mathbf{kU} + \omega', \tag{3}$$

where $\mathbf{U}$ is the solar wind speed. Increment (1) reaches its maximum for $\theta = 0$ and $k_\parallel = k_\mathrm{m} \sim \omega_{0\mathrm{p}}/c$. This is why Eqn (3) can be rewritten as

$$\omega \approx \omega_{0\mathrm{p}}\left(\frac{U}{c}\right)\cos\psi, \tag{4}$$

where ψ is the angle between vectors $\mathbf{U}$ and $\mathbf{B}$ because $\Omega_\mathrm{p} \ll \omega_{0\mathrm{p}}(U/c)$ with a large excess. For typical values $U = 4 \times 10^7$ cm s^{-1}, $\omega_{0\mathrm{p}} = 4 \times 10^3$ s^{-1}, and $\psi = 45°$, we get $\omega = 3.8$ s^{-1}. Thus, a strong Doppler shift displaces the frequency of an ion-cyclotron wave excited in the interplanetary space into the range of Pc1.

It is rather difficult to theoretically analyze the possibility of waves in the solar wind penetrating to Earth's surface, because the wave propagation path lies in a medium with an exclusively complex configuration. However, in space physics, such a possibility cannot be ruled out after the theory on the outer magnetospheric origin of ULF Pc3 waves, always observed on the Earth side turned toward the Sun [25, 26], was substantiated experimentally. Let us assume that ion-cyclotron waves can, under appropriate circumstances, penetrate into the magnetosphere from interplanetary space and be observed on Earth's surface. Thus far, we have only estimated the range of frequencies where observations should be carried out. We mention now one important distinguishing property of these waves: they should be characterized by a deep modulation of the carrier frequency.

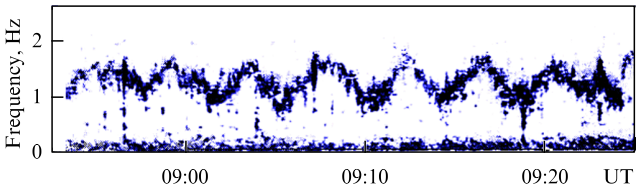

Figure 2. Dynamical spectrum of serpentine emission observed on 10.01.1968 in the southern polar cap (Vostok Observatory, Antarctica).

Indeed, the angle ψ varies strongly with time. The variations in $\psi(t)$ are caused by long-period Alfvén waves emitted by the Sun. Space-borne observations indicate that such Alfvén waves are present in the solar wind, causing variations in the angle ψ in wide limits [27, 28]. According to formula (4), ion-cyclotron waves will exhibit a deep frequency deviation.

A targeted search has led to the detection of waves of such a type in the northern and southern polar caps [29–32]. The waves were called serpentine emission because of the characteristic shape of their dynamical spectrum (Fig. 2). SE is observed in quiet geomagnetic conditions, when the parameters of the magnetosphere are relatively stable. Apparently, there is no mechanism in the magnetosphere whereby a deep SE frequency modulation can be created in such conditions. At the same time, variations in ψ take place even for a quiet solar wind flow past the magnetosphere. It is therefore pertinent to assume that the source of SE is ion-cyclotron waves always present in the interplanetary space.

2.3 Modulation of serpentine emission by helioseismic oscillations

References [17, 19, 33, 34] draw attention to the fact that a quasi-periodic 5-minute modulation is encountered more frequently among various forms of frequency modulation in SE than one would expect. For example, the modulation period of SE shown in Fig. 2 is rather close to 5 min. A natural question is whether it is related to the 5-minute permanent oscillations of the Sun's surface which are well known in helioseismology [35, 36].

From general considerations, it is plausible to assume that oscillations of the photosphere excite acoustic waves that propagate away and partly transform into Alfvén waves. The Alfvén waves are carried by the solar wind to Earth's orbit and modulate the frequency of ion-cyclotron waves that supposedly penetrate into the polar caps in the form of SE. Under quiet geomagnetic conditions, when SE is observed most frequently, the solar wind stream is stationary, and the 5-minute period of modulating Alfvén waves is preserved.

Justifying the proposed scenario is anything but simple. We limit ourselves here to a description of observations that lend support to the presence of 5-minute Alfvén waves of helioseismic origin in the solar wind [37, 38]. The task lies in relating the spectra of pulsations that were computed based on observations in two regions of space lying a large distance apart. One region was located in the solar atmosphere above a coronal hole. Field lines of the Sun's magnetic field, directing the propagation of Alfvén waves, are stretched into the heliosphere by an expanding coronal plasma. The observations were carried out with the help of a spectrograph on a

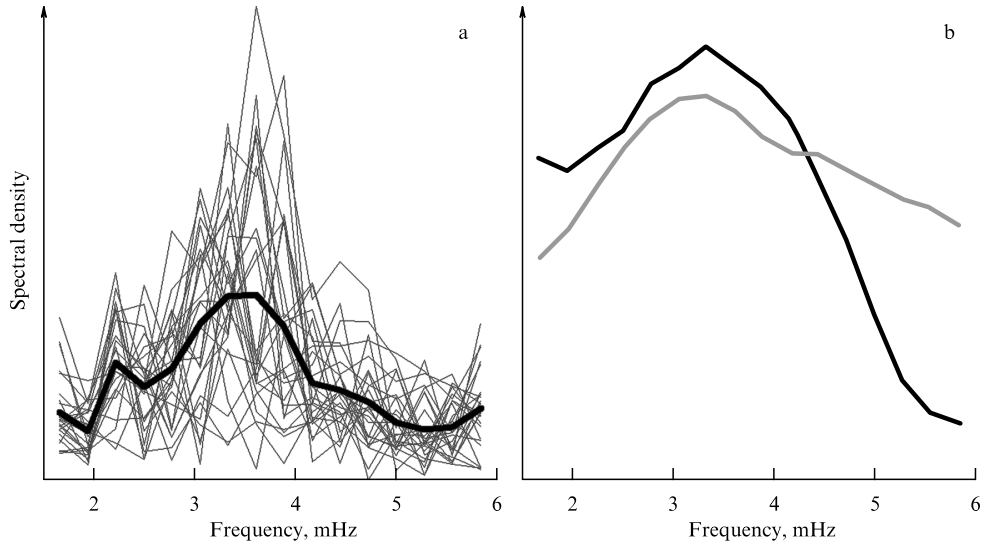

Figure 3. Comparison of the spectra of photosphere pulsations and Alfvén waves in the interplanetary space (see text).

telescope located at the Mondy Observatory. The Doppler shift of the line FeI 6569 Å with a 1-second cadence in the region of a coronal hole in the northern hemisphere of the Sun's disk was measured. The spectra of plasma velocity pulsations along the line of sight, observed for 1 h on 04.08.2005, are shown in Fig. 3a by thin lines. The spectrum averaged over 127 observational series along the entire spectrograph slit is shown by the solid line. The position of the maximum of averaged spectral density corresponds to the period of permanent helioseismic oscillations.

The second region of observations was located in the vicinity of the libration point L1 at a distance of 148×10^6 km from the Sun. The measurements were carried out with the help of the ACE (Advanced Composition Explorer) spacecraft approximately 60 h after the oscillations were observed in the photosphere, when, based on estimates, the stream of plasma from the coronal hole should reach Earth's orbit. The black line in Fig. 3b shows the spectrum of helioseismic oscillations averaged over 12 h of the observations on 04.08.2005. The gray line plots the spectrum of Alfvén oscillations based on observations in the interplanetary space. Rather satisfactory agreement between the spectra can be seen.

Alfvén waves of helioseismic origin, impinging on the magnetosphere, excite resonance oscillations of geomagnetic shells in the Pc5 range, which is convincingly demonstrated by Fig. 4 [39], which shows the spectra of Alfvén waves observed in the solar wind in front of the magnetospheric bow shock, and the spectrum of Pc5-type oscillations in the magnetosphere. This result suggests reconsidering one known observational fact: in the Pc5 range, more often than could be expected from statistical considerations relying on the continuity of the oscillation spectrum of geomagnetic shells, a period of 300 s is observed. In all probability, helioseismic oscillations manifest themselves not only in SE modulation, but also in the spectrum of classic Pc5.

It is pertinent to recall that the idea of frequency modulation was proposed by the prominent radio engineer Edwin Armstrong more than 80 years ago [40]. In the theory of frequency modulation, one distinguishes among a carrier wave, a modulating wave, and a modulated wave. In our case, this corresponds, respectively, to an ion-cyclotron wave excited in the interplanetary plasma, an Alfvén wave of solar

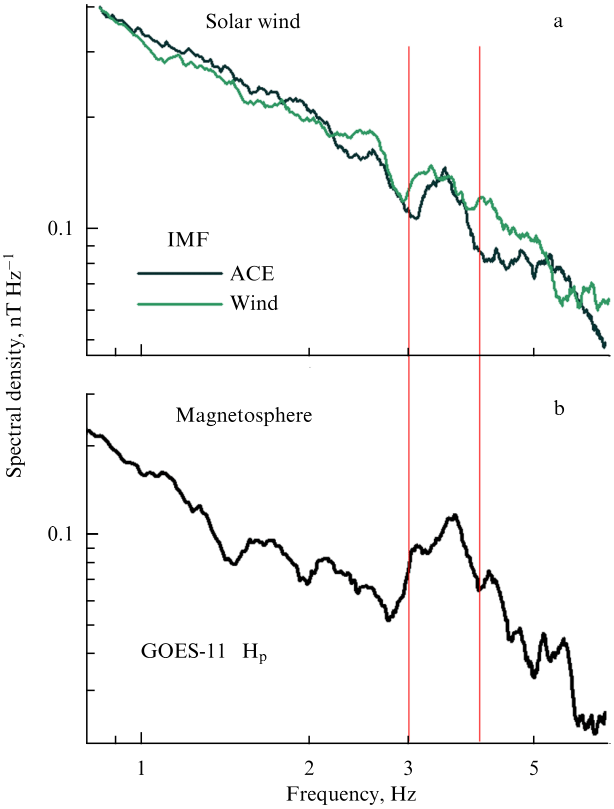

Figure 4. Daily spectra of pulsations observed simultaneously by the ACE and Wind spacecraft in the solar wind in Earth's orbit (a) and by the Geostationary Operational Environmental Satellite (GOES-11) in a geostationary orbit (b) on 13.03.2009 during a weak geomagnetic perturbation.

origin, and the serpentine emission in Earth's polar caps. In radio engineering, the modulation is done by a special circuit — a modulator, for example, a capacitor-based microphone. It is interesting to ask what plays the role of modulator in our case. It may seem strange at first glance, but the analog of the modulator is the solar wind. Indeed, the stream of solar plasma creates a strong Doppler shift, so that the information on the Sun's low-frequency oscillations is transformed into the higher frequency of serpentine emission.

We drew this parallel in order to stress an important fact, which, in essence, is as follows. Independent of the complexity of a radio circuit, we can always specify all the details of its structure and functioning. In our case, an immense distance (on the scale of wavelengths) separates the source of modulating Alfvén waves and the source of carrier ion-cyclotron waves. The distance from the 'exit of the modulator' to a receiver of frequency modulated waves in a polar cap is also large. The waves undergo complex, not always clearly understood, transformations over such distances. For this reason, we only sketched the scenario of SE generation. Many important details remain undefined.

3. Pearl necklace

3.1 Wave packet in a dispersive medium

A pearl necklace, as shown in Fig. 1, is one of the most intriguing phenomena in near-earth space. This type of Pc1 wave was discovered by Eyvind Sucksdorff [41] and Leiv Harang [42] in the middle of the 1930s at the Sodankylä (Finland) and Tromsø (Norway) observatories. The striking behavior of the amplitude-frequency modulation of pulsations, endowing the pearl necklaces with their unique character, has attracts the attention of researchers for a long time [2–4, 9, 10, 13, 43–47]. In the second half of the 20th century, a standard model for pearl waves was formulated as a result of dedicated observations and analysis, which gained wide acclaim later. The model relies on the fundamental idea of a wave packet in a dispersive nonequilibrium medium. The magnetospheric plasma is bounded, inhomogeneous, and, generally speaking, nonstationary. This would make the model too complicated. From a methodological standpoint, it is worthwhile to first assume that the medium is unbounded, homogeneous, and stationary.

A wave packet $\psi(\mathbf{x}, t)$ occupies a bounded volume in space at each given instant of time. Here, ψ is any nonzero component of a varying magnetic field. For better clarity, we begin by considering a packet propagating in the x direction in a conservative medium. To be concrete, let us take transverse electromagnetic waves with circular polarization, propagating along the field lines of a homogeneous magnetic field in a cold hydrogen plasma. We expand the packet into the superposition of plane waves:

$$\psi(\mathbf{x}, t) = \int \psi_{\mathbf{k}} \exp\left[\mathrm{i}\mathbf{k}\mathbf{x} - \mathrm{i}\omega(\mathbf{k})t\right] \mathrm{d}\mathbf{k}\,. \tag{5}$$

Here, $\omega(\mathbf{k})$ is the dispersion relation. Let the field be described by the function $\psi(\mathbf{x}, 0) = \varphi(\mathbf{x}) \exp(\mathrm{i}\mathbf{k}_0\mathbf{x})$ at the initial moment of time and let the function $\varphi(\mathbf{x})$ decay to zero fast but smoothly outside a region measuring many wavelengths, staying nearly constant inside this region. In this case, $\psi_{\mathbf{k}}$ has a sharp maximum at $\mathbf{k} = \mathbf{k}_0$, and the wave packet is quasi-monochromatic.

The sense of transition to the spectral representation (5) is that, for $t > 0$, the evolution of waves in the $\mathbf{k}$-space is trivial. Namely, each spectral component just oscillates ($\psi_{\mathbf{k}}(t) = \psi_{\mathbf{k}}(0) \exp[-\mathrm{i}\omega(\mathbf{k})t]$), whereas the frequency of oscillations $\omega(\mathbf{k})$ is given by the solution of the respective dispersion relation. (See monograph [48] for the dispersion equation for plane waves in a cold plasma.)

The subsequent steps are well known. They were made by Stokes and independently by Rayleigh in the 1870s and led to the fundamental concept of a group velocity $\mathbf{v}_\mathrm{g} = \mathrm{d}\omega/\mathrm{d}\mathbf{k}$, which is the propagation speed of a wave packet in a dispersive medium. In the same years, Umov interpreted $\mathbf{v}_\mathrm{g}$ as the propagation speed for the wave energy–momentum. If $\mathbf{v}_\mathrm{g}$ depends on frequency, it is said that the medium is dispersive with respect to the given type of wave. Note that the notion of *group velocity* was introduced by Rayleigh, whereas the notion of *dispersion* dates back to Newton.

Let us recall the derivation of the expression $\mathbf{v}_\mathrm{g} = \mathrm{d}\omega/\mathrm{d}\mathbf{k}$. We expand $\omega(\mathbf{k})$ in a series in the vicinity of $\mathbf{k}_0$ and limit ourselves to the first two terms. The first term of the expansion gives the carrier frequency of the packet $\omega(\mathbf{k}_0)$; the second term contains $\mathbf{v}_\mathrm{g}$. On inserting the reduced expansion into (5) and integrating, we conclude that the amplitude modulation $\varphi(\mathbf{x} - \mathbf{v}_\mathrm{g}t)$ propagates with velocity $\mathbf{v}_\mathrm{g}$.

In a dispersive medium, a packet spreads while propagating. The effect of spreading will be demonstrated using a one-dimensional packet as an example. For concreteness, we imagine an ion-cyclotron wave with a left circular polarization propagating in a homogeneous cold plasma strictly along a homogeneous external magnetic field. Let the envelope of the packet be Gaussian at $t = 0$, $\varphi(x) = \varphi_0 \exp[-(x/x_0)^2]$, where x is the coordinate along the packet and x_0 is the packet width. In this case,

$$\begin{aligned}\psi_k &= \frac{1}{2\pi}\int_{-\infty}^{\infty} \psi(x, 0) \exp(-\mathrm{i}kx)\, \mathrm{d}x \\ &= \psi_0 \exp\left[-\frac{1}{4}\, x_0^2 (k - k_0)^2\right],\end{aligned} \tag{6}$$

where $\psi_0 = \varphi_0 x_0 / 2\sqrt{\pi}$.

Now, keeping the first three terms in the expansion of $\omega(k)$ in powers of $k - k_0$, we integrate using (6), to get

$$\psi(x, t) = \psi_0 \exp(\mathrm{i}k_0 x - \mathrm{i}\omega_0 t) \sqrt{\frac{\pi}{\alpha + \mathrm{i}\beta t}} \exp\left[-\frac{(x - v_\mathrm{g} t)^2}{4(\alpha + \mathrm{i}\beta t)}\right]. \tag{7}$$

Here, $\omega_0 = \omega(k_0)$, $\alpha = x_0^2/4$, and $\beta = (\mathrm{d}v_\mathrm{g}/\mathrm{d}k)/2$ for $k = k_0$. It can be readily seen that the maximum of packet amplitude moves with velocity v_g and decreases with time as $(\alpha^2 + \beta^2 t^2)^{-1/4}$. The packet width increases with time as $(\alpha^2 + \beta^2 t^2)^{1/2}$. For $t > 0$, the spectral components are redistributed within the packet, such that, for $x = \mathrm{const}$, the 'instantaneous' frequency increases with time if $\beta < 0$ and decreases if $\beta > 0$. The total packet energy is preserved.

It is worthwhile to introduce the notion of group refractive index $n_\mathrm{g} = \mathrm{d}\omega n/\mathrm{d}\omega$, which in many cases allows the group velocity be conveniently expressed as $v_\mathrm{g} = c/n_\mathrm{g}$, in analogy with the expression for the phase velocity $v_\mathrm{ph} = c/n$ in terms of the ordinary refractive index. It is quite clear that $n_\mathrm{g}(\omega)$ depends on frequency in a dispersive medium.

As is known, the space plasma is not only a dispersive but also an anisotropic medium. The anisotropy comes from the presence of geomagnetic and interplanetary magnetic fields. As a result, the group refractive index depends not only on the wave frequency but also on the wave propagation direction. We, however, refrain from further details, directing the reader to monograph [48].

The law of wave energy conservation, mentioned above, is the consequence of the conservative character of an ideal medium, taken by us as a cold magnetoactive plasma. In real conditions, the waves decay and their energy is converted into heat; however, they may also be amplified if the medium is a

nonequilibrium one, as happens in the outer radiation belt, where a small proportion of energetic ions (predominantly protons) creates conditions for the onset of ion-cyclotron instability [44]. However, there is a detail which was not accounted for right away in the structure of the standard Pc1 model [2]. In the pioneering study [44], the initial perturbation was taken as a monochromatic ion-cyclotron wave propagating in an unbounded homogeneous cold plasma containing a fraction of nonequilibrium energetic ions. However, the model of a monochromatic wave occupying an unbounded space can hardly be adapted, even conceivably, to the conditions in the radiation belt. Furthermore, we will demonstrate that the radiation belt on its own cannot be a generator in any way, and acts as an amplifier of ion-cyclotron waves.

Let us take an initial perturbation as a wave packet, as we did above, instead of a monochromatic wave. We replace the frequency ω in the dispersion relation by a complex-valued quantity $\omega + i\gamma$, the imaginary part of which is usually called an instability increment of the medium with respect to wave perturbations of a given type if $\gamma > 0$, and as an instability decrement if $\gamma < 0$. Computations of γ in the framework of realistic medium models are a mathematically complicated and often rather cumbersome procedure. For us, here, it suffices to suppose that $\gamma > 0$ in some range of frequencies ω (or wave numbers k) and that $\gamma \leqslant 0$ outside that range.

Consider a wave packet of small amplitude in a nonequilibrium medium. Let us assume that the distribution of γ in the instability range is unimodal, as it usually is in many cases (see, e.g., Ref. [3]). We expand the functions $\gamma(k)$ and $\omega(k)$ in the vicinity of the maximum increment,

$$\gamma = \gamma_m - a(k - k_m)^2\,, \quad \omega = \omega_m + v_g(k - k_m) + b(k - k_m)^2\,. \tag{8}$$

Here,

$$\gamma_m = \gamma(k_m)\,, \quad \omega_m = \omega(k_m)\,, \quad a = \left.\frac{d^2\gamma}{2\,dk^2}\right|_{k=k_m}\,,$$
$$b = \left.\frac{d^2\omega}{2\,dk^2}\right|_{k=k_m}\,, \quad \gamma_m > 0\,, \quad a > 0\,.$$

Further computations, which are rather similar to those done earlier, lead to the following evolution law for a wave packet in a nonequilibrium medium:

$$\psi(x,t) = \psi_0\left[\frac{\pi}{(a+ib)t + x_0^2/4}\right]^{1/2} \times \exp\left\{i(k_m x - \omega_m t) + \gamma_m t - \frac{\left[x - v_g t + ix_0^2(k_m - k_0)/2\right]^2}{4(a+ib)t + x_0^2} - \frac{x_0^2}{4}(k_m - k_0)^2\right\}. \tag{9}$$

The amplitude of the packet increases exponentially with time owing to the transformation of the available energy of nonequilibrium plasma into wave energy.

Formula (9) allows us to see an essential distinction, important for applications, between the absolute and convective instabilities in a nonequilibrium medium [49]. In the case of absolute instability, the energy increases at any point in space. As follows from (9), this is controlled by the inequality

$$\gamma_m > \frac{v_g^2 a}{4(a^2 + b^2)}\,. \tag{10}$$

In the opposite case, the instability is convective — the amplitude stays finite at any fixed point in space. It grows exponentially only in the frame of reference moving with the group velocity, for example, at the point $x = v_g t$. Note that the ion-cyclotron instability in Earth's radiation belt has a convective character [46]. This implies that ion-cyclotron waves can be amplified within the radiation belt, but their generation is impossible.

3.2 Standard model

Thus, contrary to the commonly shared opinion, no self-excitation of ion-cyclotron waves takes place in the radiation belt, because criterion (10) is not observed. However, self-excitation is possible in an extended system which embraces the radiation belt and an open resonator. The resonator is formed by a geomagnetic field tube whose ends rest on the ionosphere in magnetically conjugate regions of the northern and southern hemispheres. A wave packet amplified in the radiation belt propagates to Earth, reaches one of the resonator ends, is partly reflected there, and enters the amplifier again, and then the process is repeated in the opposite hemisphere. If the coefficients of reflection from the ionosphere are sufficiently large, the radiation belt enters the regime of generation at the frequency of ion-cyclotron resonance

$$\omega_m = \Omega_p\left(\frac{c_A}{v_{\|p}}\right), \tag{11}$$

where Ω_p is the proton gyrofrequency at the equator of the field tube, c_A is the Alfvén speed, $v_{\|p} = \sqrt{2T_\|/m_p}$, and $T_\|$ is the longitudinal temperature of energetic protons. Here, for simplicity, we assume $c_A \ll v_{\|p}$. This is a rough outline of the standard model for the excitation of ULF Pc1 waves, described in more detail in reviews and monographs [2–4, 9, 10].

In the standard model framework, the interpretation of the dynamical spectrum of the pearl necklace presented in Fig. 1 consists of the following. In fact, we observe one and the same packet of ion-cyclotron waves oscillating along a geomagnetic field tube owing to reflections from the ionosphere in magnetically conjugate regions. The packet periodically passes through the radiation belt. The generation occurs under the condition that the energy pumped into the wave field in the radiation belt exceed the losses in reflection from the ionosphere. The repetition period for the structural elements in Fig. 1 is twice the travel time from one conjugate point to the other one with the group velocity v_g. The carrier frequency is defined by resonance condition (11). The rise in frequency within each structural element is explained by the fact that the ion-cyclotron waves undergo dispersive spreading, and the parameter of dispersion is negative, $\beta = dv_g/2dk < 0$ (see formula (7)).

An essential element of the standard model is the ionospheric magnetohydrodynamical (MHD) waveguide, along which fast magnetoacoustic waves can propagate along Earth's surface [2, 9, 45]. A fraction of the energy from the wave packet coming from above is spent on pumping the ionospheric waveguide through the conversion of the Alfvén

waves arriving from the magnetosphere into magnetoacoustic waves. The existence of the waveguide creates a possibility of observing the pearls at large distances from the place where the wave packet enters the ionosphere.

We did not specially mention this, but it should be clear from the context in any case that the analysis was based on the linear wave propagation theory. In other words, the amplitude of the initial perturbation was assumed to be sufficiently small. In an unstable medium, a wave packet evolves by law (9) only during a short time interval. The packet amplitude exponentially increases, and the linear theory becomes inapplicable past a time on the order of $1/\gamma_m$ after the process begins. A rigorous analysis of the nonlinear evolution stage is not intended here. We limit ourselves to presenting one evolution scenario which is interesting from the physical viewpoint and is possibly useful for the interpretation of observations.

On a qualitative level, small perturbations in an amplifying medium evolve according to the following scenario. When initial perturbations grow through the linear stage, their spectrum narrows rapidly, concentrating in a small vicinity of the resonance frequency $\omega_m = \omega(k_m)$. Nonlinear processes come into play as the amplitude increases. The nonlinearity is called dissipative if $\gamma(k)$ is modified under the action of waves or conservative if $\omega(k)$ is modified. We concentrate on the conservative nonlinearity and model it by adding the term $\eta|\psi|^2$ to the right-hand side of the second of formulas (8). We assume that the well-known Lighthill criterion holds, $\eta b < 0$. In this case, the wave field will undergo modulation instability. As a result, the spectrum will broaden, which will lead to the transfer of wave energy from the amplification region ($|k - k_{res}| < \Delta k$) to the region of dissipation ($|k - k_{res}| > \Delta k$). Here, Δk is the width of the amplification band. Thus, the amplitude of $|\psi|$ is stabilized because of the spectral energy transfer.

We borrowed this scenario from the theory of wind waves on water [50]. It cannot be ruled out that it may take place in a nonequilibrium plasma [51]. Let us dwell on one interesting circumstance. It is generally accepted that the modulation instability leads to the formation of solitons. It turns out that in an active (amplifying) dispersive nonlinear medium a soliton has no free parameters. Its amplitude, width, and carrier frequency are fully determined by the medium parameters. It should be recalled that in a passive medium a soliton has two free parameters, namely the amplitude and carrier frequency. The width of the soliton is determined by its amplitude. In contrast, in a linear wave packet propagating in a passive medium, the amplitude, width, and carrier frequency do not depend on each other, i.e., are free parameters.

3.3 Jump in pearl carrier frequency

There are grounds to think that the source of pearls is indeed located in the outer radiation belt and that the energy is pumped from the free energy of fast protons caught in the geomagnetic trap. Several facts testify to this. Consider one of them, since it is directly related to the topic of this review: the jump in pearl frequency that accompanies a sudden compression of the magnetosphere [4, 10].

A sudden compression of the magnetosphere follows a magnetic storm sudden commencement (SSC). On the surface of Earth, an increase ΔB in the geomagnetic field is detected, while the gyrofrequency of protons Ω_p and the density of the background plasma increase in the radiation belt. Suppose that prior to an SSC an instability condition is fulfilled in some region in the radiation belt, and pearls are excited there. The carrier frequency of oscillations is determined by the condition of ion-cyclotron resonance. One would expect that after the SSC the frequency ω would change, according to (11), by a quantity proportional to ΔB. Observations confirm this expectation.

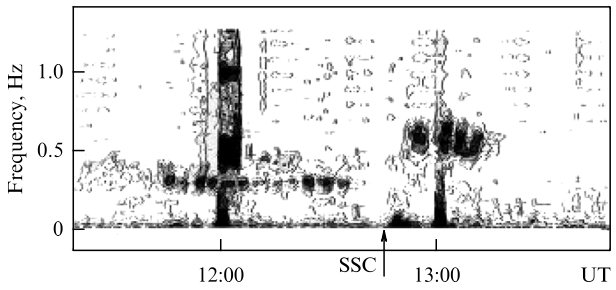

Figure 5. Jump in carrier frequency of pearls on sudden compression of the magnetosphere based on the observations from the Sodankylä Observatory (Finland), 03.10.1997. The instant of the SSC is marked by the arrow.

Figure 5 illustrates this situation. The jump in frequency is rather apparent, but there are two complications. We see a short delay in the excitation of the second part in the pulsation series relative to the first one. It is possible that the delay is in some way related to the complex structure of the front of an interplanetary shock wave of solar origin that caused the SSC on colliding with Earth's magnetosphere. Further, we see spectral broadening and apparent intensification of pulsations. This important feature in the transformation of the pulsation spectrum calls for a more thorough analysis of kinetic processes in the radiation belt.

Relative changes in quantities Ω_p, c_A, and $v_{\|p}$ can be readily expressed through ΔB. As a result, we find that the frequency increases by

$$\Delta\omega \approx 1.8\left(\frac{\Delta B}{B}\right)\omega\,. \tag{12}$$

Here, B is the magnitude of the geomagnetic field at the top of pearl wave trajectory.

We gave a relatively simple example for the change in wave frequency caused by a parametric transformation in the source frequency. However, at an earlier time, the analysis of jumps in the carrier frequency in an SSC was of fundamental significance for clarifying how pearls are excited in the outer radiation belt. Indeed, based on the data on ΔB and $\Delta\omega/\omega$, one can estimate the parameter L of the pearl trajectory with the help of formula (12) and the relationship $B = B_E/L^3$. Here, $B_E = 0.34$ G is the magnitude of the geomagnetic field at Earth's equator, and L is the geocentric distance to the top of the trajectory expressed in Earth radii $R_E = 6371$ km. It turns out that $L \sim 4$, i.e., the trajectory intersects the outer radiation belt.

A clarification is needed concerning the anisotropy of the proton temperature in the radiation belt. A two-temperature Maxwell distribution is frequently used as a plausible model for the distribution of protons over velocities. Satellite measurements indicate that $T_\perp > T_\|$. This is clear physically, because the radiation belt is formed through betatron acceleration accompanying the transfer of charged particles from the periphery to the inside of the magnetosphere (see Ref. [52] for more details). An additional clarification is required due to the fact that the conditions necessary for

cyclotron instability in the radiation belt and solar wind are opposites ($T_\perp > T_\parallel$ and $T_\perp < T_\parallel$, respectively). In the end, it comes from the fact that, in the magnetosphere, if we skip its periphery regions, we are dealing with a low pressure plasma, and in the solar wind, with a high pressure plasma.

3.4 Three problems in interpreting pearls

The beauty, elegance, and richness of the theory of wave packet propagation in dispersive nonequilibrium media are manifested in the fact that, from a limited number of standard model postulates, it turned out to be possible to logically draw a number of plausible inferences on the striking properties of pearl waves. It seemed that many, if not all, properties of pearls can be understood and described in the framework of the theory, at least on a qualitative level [2–4, 9–12, 46]. With time, however, internal inconsistencies in the standard model have become more apparent, together with its disagreement with observational facts. Finally, toward the beginning of the present millennium, the question of the need to radically revise the standard model [53] arose sharply.

This section describes this dramatic situation. It attracts the interest of many researchers. In 2006, a special session of the General Assembly of the European Geosciences Union (EGU) in Vienna was devoted to the actual problems with describing pearls [https://meetings/copernicus.org/egu2006/]. A special issue of a renowned international journal [54] was dedicated to the analysis of various hypotheses on the pearl's origin [55], a comparison of satellite and terrestrial observations of electromagnetic waves in the Pc1 range [56], and the consideration of the interaction between Pc1 and other form of oscillations [57, 58] and streams of charged particles [59]. Interest in the riddles of pearl waves is not ceasing. In recent years, satellite measurements [60, 61] and their theoretical interpretation [62–64] have garnered a particular attention.

We concentrate on the main unsolved issues. First of all, we note that the slope of structural elements in the series of pearls shown in Fig. 1 does not change with time. Generally speaking, this contradicts the linear theory suggesting a broadening of wave packets. The theory predicts that the slope of elements to the time axis must increase monotonically if we are really dealing with one and the same wave packet oscillating along geomagnetic field lines between the conjugate points in the southern and northern hemispheres. An attempt has been made to explain the stability of the structural element slope in the framework of quasi-linear plasma stability theory [65–67]. But the problem cannot be considered solved, because it is not clear how the proposed hypothesis on the origin of anomalous pearl dispersion can be experimentally confirmed or rejected.

We will call the second problem the problem of discrete shape. Its essence is that in the framework of linear theory for waves in a dispersive nonequilibrium media there is no mechanism that would stratify the dynamical spectrum in the way shown in Fig. 1. As in the case with anomalous dispersion, we need to augment the standard model by a hypothesis that a nonlinear mechanism is responsible for the formation of a quasi-periodic set of structural elements. Sometimes, the structural element in a series of pearls is referred to as a soliton, but this is noting more than only the general direction of thought in searching for a solution to the problem of discrete shape. There is no physical content in the analogy between a pearl and a soliton.

The problem of discrete shape and the problem of pearl dispersion can be seen as theoretical ones in the sense that

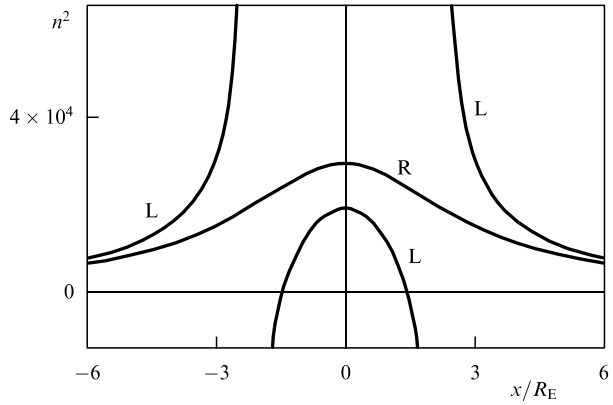

Figure 6. Squared refractive index for electromagnetic waves with left (L) and right (R) circular polarization. The horizontal axis corresponds to the distance along a geomagnetic field line crossing the outer radiation belt. The ion-cyclotron resonator is located between the reflection points for the L-wave.

observations tell us about well defined and stable properties of pulsations, whereas theory appears to be insufficiently elaborate to explain these properties. Moreover, most likely, both problems are in the realm of the theory of nonlinear pulsations. In contrast, the third problem to be mentioned here, first, is an experimental one, and second, can be fully formulated in the framework of the theory of linear propagation of ion-cyclotron waves. We call it the problem of the existence of ion-cyclotron resonators (ICRs) in the magnetosphere. Indeed, the theory unequivocally points to the existence of ICRs, but we did not manage to find experimental confirmation, despite all our efforts in this direction [12, 53, 68–70].

The problem of ICRs arises because of the presence in the magnetosphere of a small fraction of heavy ions (for example, O^+). A specific inhomogeneity of the geomagnetic field in the vicinity of the equatorial plane plays a key role in the formation of ICRs. A hypothesis on the existence of ICRs is illustrated in Fig. 6. We see that two adjacent zeros of the refractive index of ion-cyclotron waves are located on both sides of the equator of a geomagnetic field line passing through the radiation belt. An ICR is supposedly located between them. We give only this brief explanation (see review [12] for details).

The main distinction between ICRs and a resonator of the standard model of pearl self-excitation is that the reflection points lie not in the ionosphere, but high over Earth, in the near vicinity of the top of the geomagnetic field line, which is the resonator axis. In this respect, there is an additional problem of interpretation, since it is not clear how the energy of waves accumulated in ICRs is carried to Earth.

Interestingly, the period of wave packet oscillations between the ends of an ICR is approximately equal to the repeat period of structural elements in the pearl series. Moreover, a linear wave packet in an ICR does not broaden, even though it propagates in a dispersive medium [68]. This partly solves the first interpretation problem mentioned by us. It is still not fully clear why we commonly observe signals with a rising tone and not, for example, a falling tone. The idea of ICRs, the existence of which is convincingly supported by theory, helped in understanding one of the fundamental properties of pearls — a strict anticorrelation of the appearance of this type of pulsation with the Sun's 11-year activity

cycle. Namely, we succeeded in relating this behavior to the 11-year solar-cyclic variation in the density of heavy ions O^+ in Earth's magnetosphere [12, 68]. And yet, the theory of ICRs, being linear, gives no hints concerning the stratification of the dynamical spectrum, distinctly seen in Fig. 1.

We have seen how complicated the interpretation of ULF electromagnetic waves of natural origin can be. Many tens of space physicists equipped with a highly advanced theory of wave propagation in dispersive nonequilibrium media have not succeeded in solving the riddle of pearl waves over almost half century of intense research. In our opinion, the problem of discrete signal shape is the most difficult one. In order to find at least some approach to its solution, we turn to the theory of critical phenomena, beginning with the Landau phenomenological theory, having adapted it to our case.

Let us introduce an order parameter $\varepsilon = |\psi|^2$ proportional to the wave energy density in the center of an ICR, averaged over a certain time interval as needed. The evolution equation takes the form

$$\frac{\mathrm{d}\varepsilon}{\mathrm{d}t} = 2\Gamma\varepsilon\,. \tag{13}$$

The nonlinear increment $\Gamma(\Lambda, \varepsilon)$ is expressed as

$$\Gamma(\Lambda, \varepsilon) = \gamma(\Lambda) - \alpha\varepsilon\,, \tag{14}$$

where α is the Landau constant, and Λ is a governing parameter [71]. (Do not confuse the Landau parameter with the parameter α in formula (7).) Close to the self-excitation threshold, the linear increment $\gamma(\Lambda)$ is proportional to the governing parameter,

$$\gamma(\Lambda) = \beta(\Lambda - \Lambda_\mathrm{c})\,. \tag{15}$$

Here, Λ_c is some critical value of Λ, and β is the proportionality coefficient. The theory of ion-cyclotron instability of the radiation belt [10, 44] suggests that the choice of the governing parameter is $\Lambda = N'(T_\perp/T_\parallel - 1)$, where N' is the concentration of energetic protons. Thus, the theory contains three phenomenological parameters, α, β, and Λ_c.

In the state of equilibrium, $\mathrm{d}\varepsilon/\mathrm{d}t = 0$. The equilibrium can be disordered, when $\varepsilon = 0$, or ordered, when $\varepsilon \neq 0$ for $\Gamma(\varepsilon, \Lambda) = 0$. An important aspect is the sign of α in expression (14) for the nonlinear increment. If $\alpha > 0$, one is dealing with a system with soft excitation of pulsations, and the excitation is hard if $\alpha < 0$. A quasi-linear theory for the interaction of waves and particles in the radiation belt predicts $\alpha > 0$. Apparently, it is difficult to expect that the discrete pearls will be formed in a soft regime. Indeed, a system with soft excitation is characterized by a disordered state for $\Lambda < \Lambda_\mathrm{c}$, and an ordered one for $\Lambda > \Lambda_\mathrm{c}$. In the second case, pulsations are excited under the action of arbitrarily small perturbation, and regular intervals between risings observed in a pearl necklace cannot be formed.

In this respect the regime of hard excitation would be more interesting [4]. In contrast to a dynamical system with soft excitation, a system with hard excitation is meta-stable in its subcritical state. In other words, it is stable with respect to infinitesimal perturbations, but can switch to a self-oscillatory regime under the action of a trigger, i.e., a perturbation with a finite, even if small, amplitude. However, concrete mechanisms that would maintain a hard regime have not been found in the radiation belt yet.

In our opinion, an interesting and promising avenue is the development of a theory relying on the idea of an inflow-based resonator [72]. We were discussing earlier a resonator in the standard model of pearls; however, a powerful *idea of inflow* is without a doubt applicable also to ICRs. Consider the following situation. The lateral walls of an open resonator are formed by a system of caustics, i.e., they are fully transparent to ions of the radiation belt that drift from west to east in the inhomogeneous geomagnetic field. Thus, the ICR is 'ventilated' by a flow of hot particles that possess some surplus of free energy. Outside the resonator, the free energy does not transform into wave energy because the instability of particle distribution in the radiation belt is convective. However, such a transformation is possible inside the resonator, and, under certain conditions, wave self-generation takes place. The quasi-linear interaction of waves and particles in the ICR leads to a reduction in free energy, but the inflow of new particles replenishes the losses. It turns out that the current value of the nonlinear increment Γ in an inflow-based resonator depends on the history of the wave field evolution. Formally, this circumstance is expressed as follows:

$$\Gamma(\Lambda, \varepsilon, t) = \gamma(\Lambda) - \eta\int_{-\infty}^{t} \varepsilon(t')\,\Phi(t' - t)\,\mathrm{d}t'\,. \tag{16}$$

It has been shown in [72] that the wave field is split into a periodic sequence of discrete signals if the form-factor $\Phi = 0$ for $t' < t - \tau$ and $\Phi = 1$ for $t - \tau \leqslant t' \leqslant t$. Here, τ is the time an energetic particle from the radiation belt traverses the ICR. A rough estimate of τ coincides with the pearl repetition period.

The idea of an inflow-based resonator was picked up by other researchers and saw some development on a phenomenological level in a series of studies [73–77]. There was no success constructing a working microscopic theory, so the question of the mechanism whereby the pearls are discrete is still open. It is only clear that the discrete character of pearls, noted already by Sucksdorff in his pioneering paper [41], is incompatible with the standard theory of pearl origin.

We propose a speculative consideration which will possibly shed some light on the origin of risings in a series of pearls (see Fig. 1). Let us assume that, for one reason or another, $\Gamma = 0$ and $\varepsilon = 0$ at $t = 0$. This may happen as a result of wave field evolution according to Eqns (13) and (16). At the moment $t = 0$, no pulsations are excited. However, at $t > 0$, new energetic ions from the radiation belt drifting from the west to the east and carrying an excess of free energy start to arrive at the resonator. (Namely this is the essence of an inflow-based ICR.) As the resonator becomes filled, the process of self-excitation is resumed. Obviously, more energetic particles fill the ICR faster than do less energetic particles. Yet, this implies that pulsations of a relatively low frequency will be excited somewhat earlier than those of a higher frequency, in agreement with resonance condition (11). In other words, the frequency increase in a structural element is related to the particle distribution over velocities and not the wave packet spreading. One can readily see that $\omega \propto \sqrt{t}$, i.e., that the function $\omega(t)$ is convex within a rising, which is commonly observed experimentally.

We carried out an analysis of open problems in the physics of magnetospheric Pc1 waves, demonstrating that the development of new ideas is needed outside the framework of the standard model in order to understand the intriguing properties of the dynamical pulsation spectrum.

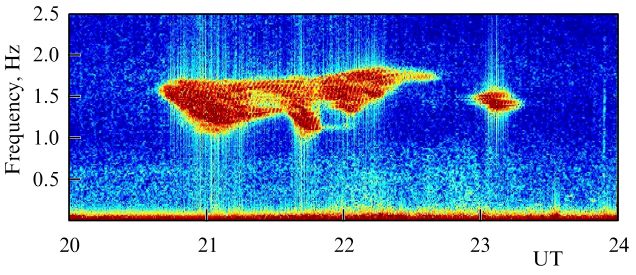

Figure 7. (Color online.) Spectrogram of a pearl with a complex structure observed at the Mondy Observatory on 13.11.2015.

Generally speaking, the treatment of the range of questions to be explored testifies to the successful development of one domain of research or another. And yet, the problems with Pc1 we mentioned have remained open so long that this already begins to be disturbing. We believe that, in the end, the mechanism behind the formation of stable wave structures observed on Earth and in space as pearl necklaces will be uncovered through joint efforts. Our hope relies, first of all, on the idea of an inflow ion-cyclotron resonator located in the equatorial vicinity of the outer radiation belt.

We conclude this section by presenting Fig. 7, demonstrating an evolution of pearls. For 2.5 h, we witness a picture of mighty processes unfolding in the radiation belt. It is likely that we are observing the action of several pulsation sources. Most surprising is the stability of the morphological shape of the pearls. We clearly distinguish an edgy structure in the form of a periodic sequence of signals with an ascending tone. This universal behavior has thus far defied physical explanation.

4. Discrete signal

4.1 Green's function of the propagation path

The term modulation is commonly used for a slow and smooth variation in wave field parameters. In Section 3.1, we selected the initial condition $\psi(x,0)$ such that the wave packet undergoes modulation for $t \geqslant 0$. If, in contrast, the initial perturbation is taken arbitrarily, for example, as a sharp impulse, then the initial evolution of the wave field will be neither slow nor smooth. Only with time will an impulse in a dispersive medium be transformed into an amplitude-frequency modulated wave.

As an illustration, consider waves propagating in the positive direction of the x-axis in a homogeneous, unbounded, and conservative medium. Let an arbitrary initial perturbation $\psi(x,0)$ be given at $t = 0$. We need to find the wave shape at $t > 0$. The exact solution is quite similar to (5). However, now we do not assume that the spectrum of the initial impulse is narrow, and therefore cannot use the expansion of $\omega(k)$ in powers of k. The solution remains formal, in the sense that it does not give a clear idea on the evolution of the initial impulse until the respective integral is computed. We make use of the stationary phase method and compute the integral asymptotically for $t \to \infty$,

$$\psi(x,t) = \psi_k(0)\sqrt{\frac{\pi}{|\beta(k_s)|t}} \times \exp\left\{\mathrm{i}\left[k_s x - \omega(k_s)t - \frac{\pi}{4}\operatorname{sgn}\beta(k_s)\right]\right\}. \qquad (17)$$

Here, k_s is found from the condition that the phase be stationary, $v_g(k_s) = x/t$.

Thus, at large distances and for large times, an initially broadband impulse is transformed into a modulated quasi-sinusoidal wave. Its amplitude decays with time as $1/\sqrt{t}$. The spectral components $\psi_k(0)$ of the initial impulse propagate along the family of world lines $x = v_g(k)t$ in two-dimensional space–time (x,t). In other words, the asymptotic form contains a pack of trajectories of rays fanning out in space–time, and the spectrum of the initial impulse 'spreads out' along them [78, 79].

We considered a Cauchy problem when the wave field structure is specified in the entire space at some initial time moment. From the geophysical standpoint, a boundary-value problem is also of interest: at the point $x = 0$, a signal $\psi_k(0,t)$, $-\infty < t < \infty$ is given; we need to find the signal $\psi_k(x,t)$ at the observation point $x > 0$. The interval $[0,x]$ will be referred to as the propagation path.

A boundary-value problem arises, for example, in studying interfering radio signals from lightning discharges. The propagation path in this case is the part of the earth–ionosphere waveguide or an interval of the geomagnetic field line that connects the lightning discharge with a detector. The detector can be located on the surface of Earth or in the ionosphere (on a spacecraft). In the ULF range, the boundary-value problem arises in relation to the outer-magnetospheric origin of some kinds of waves. A source can be located in the geomagnetic tail, in the interplanetary medium in front of the magnetospheric bow shock, and on the Sun's surface. In the last case, the path is located in interplanetary space between the Sun and Earth.

The solution to the one-dimensional boundary-value problem for the half-space $x \geqslant 0$ is given by the Fourier integral

$$\psi(x,t) = \int_{-\infty}^{\infty} \psi_\omega(0)\exp\left[\mathrm{i}k(\omega)x - \mathrm{i}\omega t\right]\mathrm{d}\omega\,, \qquad (18)$$

where $k(\omega)$ is a branch of the dispersion equation that corresponds to the type of normal waves which propagate from the source to the point of observation. The source frequency spectrum $\psi_\omega(0)$ is determined by the form of signal $\psi(0,t)$ given at the boundary $x = 0$. If the perturbation is carried along the path by several types of normal waves, then solution (18) with the appropriate dispersion law $k(\omega)$ has to be written for each of them, with subsequent summation over all such solutions.

Of special interest is the case where a δ-impulse enters the propagation path. In this case, solution (18) is called the Green's function or pulse response of the propagation path and is written as

$$G(x,t) = \frac{1}{2\pi}\int_{-\infty}^{\infty} \exp\left[\mathrm{i}k(\omega)x - \mathrm{i}\omega t\right]\mathrm{d}\omega\,. \qquad (19)$$

The Green's function fully characterizes the propagation path. If one succeeds in finding $G(x,t)$, then, computing the response of the path to an arbitrary input signal is relatively straightforward [78].

However, finding the Green's function is far from simple, even for a homogeneous domain. An asymptotic estimate can be obtained by the stationary phase method, similar to how it was done earlier when solving the Cauchy problem. The stationary points $\omega = \omega_s$ are found by solving the equation

$$v_g(\omega_s) = \frac{x}{t}\,, \qquad (20)$$

where $v_g = c/n_g$, $n_g = d\omega n/d\omega$, and $n = ck/\omega$. We compute further the first term in the asymptotic expansion of integral (18). It has a form analogous to (17), but the length of the path x, in contrast to that in the case of (17), is fixed, which corresponds to typical conditions of geophysical observations. In this case, one cannot speak about spatiotemporal rays $x/t = \text{const}$, $t \to \infty$, $x \to \infty$. Instead, one is dealing with the asymptotic form of the spectral-temporal representation of the Green's function. The idea is as follows.

At the exit of a path with fixed but large length x, an impulse signal presents a quasi-monochromatic wave with a slowly varying amplitude and frequency. An 'instantaneous' carrier frequency satisfies condition (20), or

$$t = \frac{x}{c}\, n_g(\omega)\,, \tag{21}$$

which is the same thing.

Consider the plane $\omega - t$ and plot points satisfying (21). They form a system of lines aligned with the 'crests' of the Green's function. Such a system is referred to as a dynamical spectrum. It can be made more elaborate if we plot on the $\omega - t$ plane not only the 'crests' but also other elements of the spectral-temporal 'relief.' If the propagation domain is smoothly inhomogeneous, then, instead of (21), in the Wentzel–Kramers–Brillouin (WKB) approximation we have

$$t(\omega) = c^{-1} \int_0^x n_g(\omega, x)\, dx\,. \tag{22}$$

This is the most important characteristic of the propagation path. It is called the signal group delay time.

In geophysical research, the dynamical spectrum $\Gamma(\omega, t)$ of the Green's function is commonly computed through the following construction. The spectrum of the Green's function is multiplied by $2\pi \exp[-\alpha(\nu - \omega)^2]$, i.e., a window with a width of $\alpha^{-1/2}$ centered at the frequency $\nu = \omega$ is applied to the spectrum. After this, the inverse Fourier transform is carried out,

$$\Gamma(\omega, t) = \int_{-\infty}^{\infty} \exp\left[-i\nu t + i\,\frac{x}{c}\,\nu n(\nu) - \alpha(\nu - \omega)^2\right] d\nu\,. \tag{23}$$

For sufficiently large α, the main contribution to the integral comes from frequencies ν that are close to ω. We introduce the notation $\xi = \nu - \omega$ and expand $n(\nu)$ in a series in powers of ξ with an accuracy up to the quadratic term. The result is

$$\Gamma(\omega, t) = \int_{-\infty}^{\infty} d\xi \exp\left\{ i\xi\left[\frac{x}{c}\, n_g(\omega) - t\right] + \frac{\xi^2}{2}\left[i\,\frac{x}{c}\,\frac{dn_g}{d\omega} - \alpha\right]\right\}, \tag{24}$$

or, after integration,

$$\Gamma(\omega, t) = \sqrt{\frac{2\pi}{\alpha - i\tau'(\omega)}}\, \exp\left\{-\frac{\left[t - \tau(\omega)\right]^2}{2\left[\alpha - i\tau'(\omega)\right]}\right\}. \tag{25}$$

Here, $\tau = (x/c)n_g$ and $\tau' = d\tau/d\omega$. Obviously, the function $|\Gamma(\omega, t)|$ reaches its maximum at $t = \tau(\omega)$. If the dispersion law $n(\omega)$ is known, formula (25) enables computations of the dynamical spectrum of a signal from an impulse source propagating through a homogeneous domain. With the help of the WKB method, expression (25) can be generalized to smoothly inhomogeneous propagation domains.

4.2 North–south asymmetry of discrete signals

The Green's function of the propagation path is widely used in one form or another in geophysics in studies of discrete frequency-modulated signals of impulse origin. An outstanding result was obtained in his time by Storey [80], who for the first time estimated the density of the exosphere by the dispersion of whistler atmospherics generated in the radio range after lightning discharges (see review [7]). Carpenter [81] discovered the plasmapause — one of the most important formations in the magnetosphere — as a result of analyses of so-called knee whistlers (see monograph [8] and references therein).

In the ULF range, isolated discrete signals (DSs) appear sporadically in the polar caps in relatively quiet geomagnetic conditions. They are the Pi1 type. The duration of an individual signal is about 3 min. Most frequently, signals of a falling tone are observed ($\tau' < 0$), and the typical parameter of dispersion is approximately $df/dt = -0.1$ Hz min^{-1}. Sometimes, signals of rising tone are also observed ($\tau' > 0$). It should be mentioned that DSs are observed relatively rarely: they occur once every 4 days on average.

Judging by the fact that DSs are observed in the polar caps and also by substantial dispersion, the signals propagate along rather long high-latitudinal paths. The position of the DS source is not known reliably. An impulse source can be located, for example, in the geomagnetic tail at a large distance from Earth. It is known that the tail is characterized by explosive energy releases during sporadic reconnections of geomagnetic field lines which, as is well known, have mutually opposite directions in the northern and southern halves of the tail [9]. Propagating to Earth along the tail as along a tube, an impulse signal may reach a polar cap, dispersively spreading out on this path. A theory describing the geomagnetic tail as a waveguide for fast magnetoacoustic waves was proposed in Ref. [82]. Computations show that DSs of falling tone are formed in the Pi1 range on paths of this type, i.e., $\tau' < 0$.

However, DSs can also be generated in front of the magnetospheric bow shock, in the region of the so-called foreshock [83, 84]. We consider this interesting possibility in more detail.

Figure 8 plots meridional sections of the magnetosphere. The position of the near-earth bow shock is shown by the dashed line. The straight lines depict the field lines of the IMF. A dichotomic variable $\sigma = \text{sgn}\,(B_x B_z)$ depends on the orientation of the IMF lines relative to the plane of the geomagnetic equator, as is apparent from the figure. The foreshock is located between the bow shock and the field line tangent to it. According to measurements from spacecraft, MHD impulses are spontaneously generated in the foreshock region [85]. They are blown by the solar wind into the magnetosphere, where they can penetrate into the polar caps and be observed as DSs.

The idea is as follows. It is obvious from geometric considerations that DSs will be observed in the northern (southern) polar cap for $\sigma = 1$ ($\sigma = -1$) if the hypothesis on the position of the source in the foreshock is valid. This gives us a rather straightforward procedure to test our hypothesis.

The north–south asymmetry in the appearance of DSs as a function of σ was discovered in Ref. [84]. Figure 9 presents the result of the study. The horizontal axis corresponds to the argument of the function σ. The dark gray histogram depicts the distribution of events by the magnitude of parameter $B_x B_z$, where B_x and B_z are the components of the IMF in front of the magnetospheric bow shock in the solar-magneto-

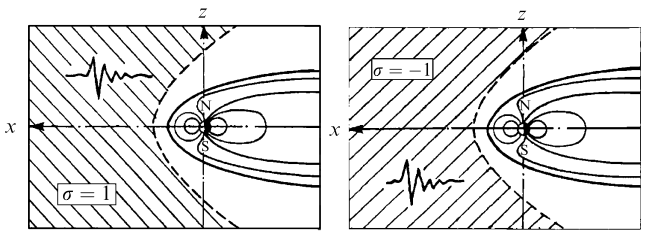

Figure 8. Section of the magnetosphere by the plane of the noon meridian for different values of dichotomic variable $\sigma = \mathrm{sgn}\,(B_x B_z)$.

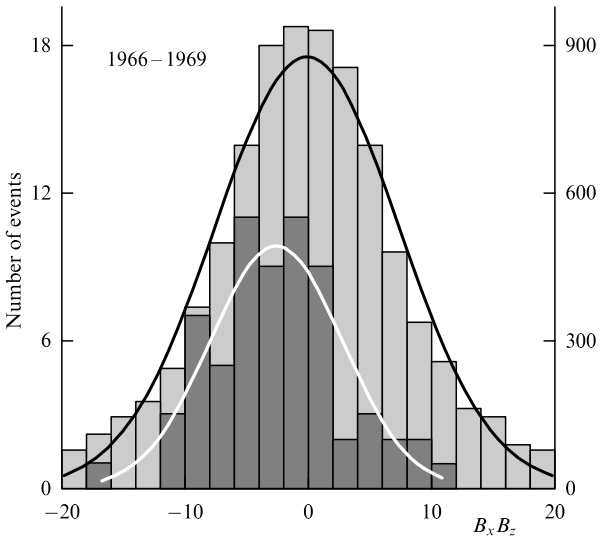

Figure 9. Distribution of events over the value of the parameter $B_x B_z$ by observations at the Vostok Observatory located in the southern polar cap. The left axis is related to DSs (dark gray histogram). The right axis corresponds to hours of magnetometric observations (gray histogram).

spheric reference plane. An event is an hour of world time, during which at least one DS of falling tone has been observed. The gray histogram shows the distribution of all those hour intervals during which ULF waves were recorded at the Vostok Observatory during polar expeditions of the IPE AS USSR at the end of the 20th century.

We see that the distribution of hours where the ULF waves were observed is symmetric around zero, whereas the distribution of DS exhibits a strong asymmetry. Namely, in the southern cap, the number of a DS for $\sigma = -1$ exceeds by more than two times the number of a DS for $\sigma = 1$. A rather similar result has been obtained by us based on observations in the northern polar cap (Thule Observatory, Greenland). Here, an asymmetry in the appearance of the DS is also observed, but with the opposite sign.

Our hypothesis is thus partially confirmed. A substantial part of the DS penetrates into the magnetosphere from the foreshock region. We can also suppose that part of the DS is excited in remote regions of the geomagnetic tail. Pulse sources of DSs generated in the tail may occur in sporadic reconnections of geomagnetic field lines having opposite directions in the northern and southern halves of the tail.

5. Pulsations of rising frequency

A significant contribution to the physics of ULF pulsations in the magnetosphere was made by domestic geophysicists, who discovered and studied in detail pulsations of rising frequency

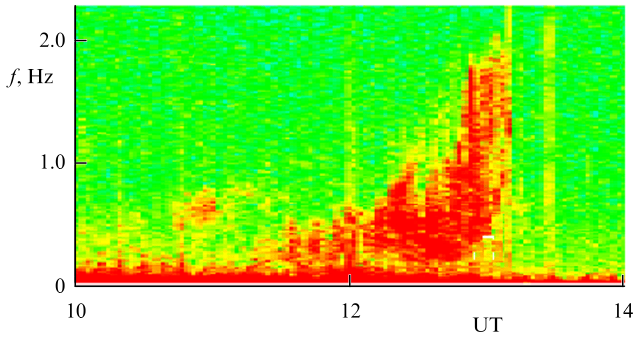

Figure 10. (Color online.) Intervals of pulsations with a decreasing period recorded at the Borok Observatory on 22.11.1997.

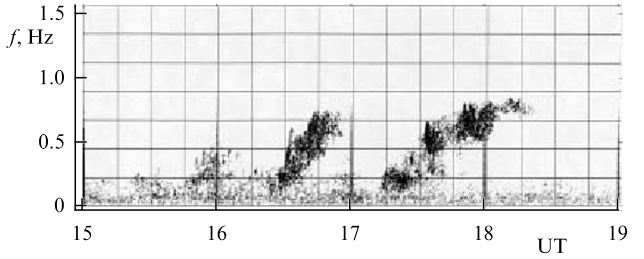

Figure 11. Example of triple excitation of pulsations with increasing frequency by observations at the Sodankylä Observatory (Finland) on 08.03.1993.

that invariably accompany geomagnetic storms [86–91]. These pulsations are widely known in the English-language literature as intervals of pulsations of diminishing period (IPDPs). Being excited during the main storm phase, IPDPs reflect the most powerful and dynamic processes in the near-Earth space.

Figure 10 gives an idea of IPDPs. Pulsations were recorded at the mid-latitude Borok Observatory during the main phase of a geomagnetic storm [92]. For 1.5 h, the frequency of oscillations monotonically increases from some fractions of a hertz to 2 Hz. We draw attention to the sign of the second time derivative of mean frequency: $\mathrm{d}^2 f/\mathrm{d}t^2 > 0$. In contrast, in Fig. 11, we see an IPDP event in which $\mathrm{d}^2 f/\mathrm{d}t^2 < 0$. The pulsations were observed at the high-latitude Sodankylä Observatory [10]. The experience gained in observations of IPDPs indicates that most probably we are dealing with two different mechanisms forming the frequency modulation of pulsations [93, 94].

We present briefly a modern view on the origin of IPDPs. We rely on the extensive literature cited in monographs and reviews [3, 4, 9, 10, 46, 51, 92–95], but will not go into details of theoretical developments. We begin by pointing out the two most important factors whose action spawns a geomagnetic storm: the dynamical pressure of the solar wind and the interplanetary electric field **E**. It should be apparent that high-speed streams of solar wind with an enhanced plasma density, ejected by solar flares and coronal holes, lead to an increased energy flux through a transverse section of the magnetosphere. As concerns the field **E**, its magnitude and orientation essentially define the efficiency of solar wind energy transfer into the magnetosphere. In other words, **E** plays the role of a certain governing parameter. A storm unfolds for an enhanced solar wind velocity if the component E_y in the solar-magnetospheric reference frame exceeds a critical value, which is approximately 1 mV m^{-1} [96].

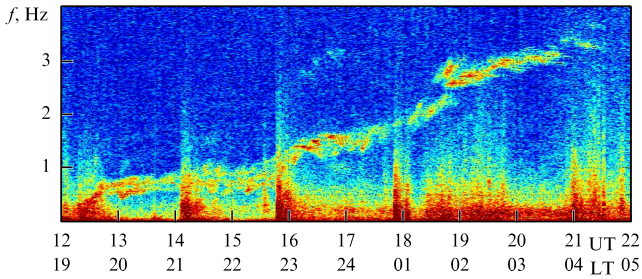

Figure 12. (Color online.) Pulsations of increasing frequency with anomalously long duration (Mondy Observatory, 17.03.2013). LT means local time.

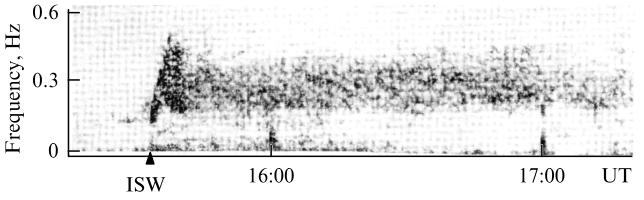

Figure 13. Dynamical spectrum of ULF radiation after the action of an interplanetary shock wave (ISW) on the magnetosphere (Vostok Observatory, 18.07.1965).

During a storm, the large-scale electric field abruptly increases in the magnetosphere, causing plasma convection and leading to the radial displacement of protons in the outer radiation belt in the direction of Earth. Protons undergo betatron acceleration, the anisotropy of their angular distribution increasing, which may result in cyclotron instability manifested as IPDPs. This is a scenario for the excitation of convective-type IPDPs. The increase in the frequency of pulsations is explained by the radial drift of radiating particles into the region of stronger magnetic field when the electric field of magnetospheric convection is increasing.

In the second scenario, describing the excitation of injective-type IPDPs, the key moment is the azimuthal, not radial, drift of energetic protons. The situation is as follows. During a storm, there are sporadic impulse injections of energetic protons and electrons from the tail into the closed geomagnetic shells. After an injection, electrons drift azimuthally eastward, and protons westward, forming the so-called circular current of the main storm phase. Injections take place in the vicinity of the midnight meridian. The velocity of azimuthal drift is proportional to particle energy. For this reason, a nonmonotonic distribution of protons over energies is formed in the evening sector of the magnetosphere. The nonmonotonic distribution can be unstable to perturbations in the Pc1–2 range, leading to the excitation of IPDPs. The increase in pulsation frequency is explained by progressively slower particles entering the evening sector of the magnetosphere with time.

From resonance condition (11), an estimate $f \propto \sqrt{t}$ follows for injective-type IPDPs. Thus, the injective IPDPs have two characteristic properties: $\mathrm{d}^2 f/\mathrm{d}t^2 < 0$ and the appearance in the evening sector. Both properties are manifested in the third IPDP in Fig. 11. However, it is rather likely that in this case the excitation of all three IPDPs occurred through three injections of energetic protons from the tail into the magnetosphere.

To conclude, we present in Fig. 12 a rare case of frequency modulated ULF pulsations [97]. In the lower part of the dynamical spectrum, one sees powerful surges of Pi1, testifying to multiple events when energetic particles were injected into the magnetosphere. Higher, in the Pc1 range, one sees an IPDP event of anomalously long duration. The total duration of oscillations is 10 h, which is several times longer than the typical IPDP duration. The maximum frequency reached is 3.5 Hz, which is also considerably higher than ordinary values. Judging by the appearance time, and also by the sign of $\mathrm{d}^2 f/\mathrm{d}t^2$, which can be judged by individual fragments, we are dealing with convective-type IPDP.

6. Discussions

We considered simple and physically transparent mechanisms of frequency modulation: Doppler modulation (see Section 2), dispersive broadening of wave packets (see Section 3) and impulses (see Section 4), and the nonstationarity of the source of pulsations (see Section 5). This could be augmented by the frequency transformation of a wave propagating in a nonstationary medium. However, we are not aware of observations of ULF waves that would directly point to the manifestation of this physically very interesting effect [79]. Rather complicated mechanisms of nonlinear transformations in wave field spectral compositions are also left outside this review. We mention here the hypothesis of a quasi-linear mechanism, whereby frequency modulation of ion-cyclotron waves is formed in the radiation belt [65, 98, 99]. Other examples can be found in monographs [3, 4] and review [100].

We focused our attention on the short-wave part of the ULF range. Here, the manifestations of frequency modulation are most vivid and variable. Indeed, in addition to the consideration above, we give two more examples. The first is shown in Fig. 13. We see a Pi1 impulse excited on collision of the magnetosphere with an interplanetary shock wave (the moment of collision is marked with a triangle). There are grounds to suppose that a powerful impulse of a rising tone, appearing at the moment of contact, presents the result of action of the oscillatory structure of the interplanetary shock wave front on the magnetosphere. A broad band in the Pc1–2 range that follows Pi1 likely reflects fluctuations of the IMF in turbulent plasma behind the shock front.

The second example is no less interesting [101]. Figure 14 depicts a diurnal variation of resonant frequencies for one of the Pc1 varieties — so-called ionospheric Alfvén resonances (IAR). The spectrum of IARs is largely defined by the concentration of electrons in the ionospheric F-layer. Earth's rotation around its axis implies that a magnetometer records oscillations with frequencies that vary with time in agreement with daily variations in the concentration of electrons in the F layer (see review [14] and references therein). Thus, an illusion that the frequency varies with time arises, because spatial modulation of the frequency of ionospheric resonances is scanned. Figure 14 illustrates this situation. The local noon is marked by the arrow.

For completeness, we touch on the question of the modulation of long-wave pulsations. As a rule, here we are dealing with a parametric modulation of respective oscillatory systems. For example, according to [25, 26], the carrier frequency of Pc3 pulsations satisfies the relationship $f = gB$ in which $g = 5.8 \pm 0.3$ mHz nT^{-1}, and B is the absolute value of the IMF. Natural variations in B lead to the modulation of the Pc3 frequency. In the Pc4–5 range, predominantly toroidal and poloidal pulsations of geomagnetic cells are

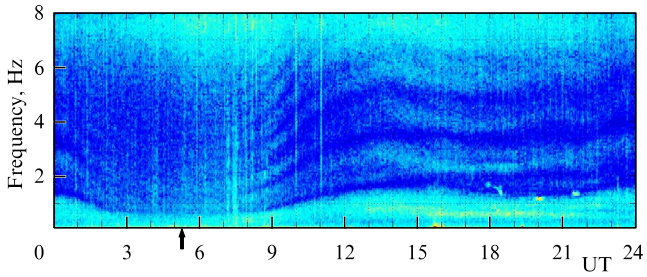

Figure 14. (Color online.) Daily spectrogram of oscillations of an ionospheric Alfvén resonator (Mondy Observatory of the Institute of Solar-Terrestrial Physics SB RAS, 02.12.2017).

observed [9, 102]. The period of pulsations depends on the size of the magnetosphere, which varies depending on the dynamical pressure of the solar wind. In Section 2.3, we paid attention to the fact that there is an interval with a certain rigidity in the spectrum of Pc5. Namely, variations in the solar wind dynamical pressure are accompanied by a more or less stable increase in spectral density at the frequency of 3.3 mHz, which coincides with the frequency of 5-minute pulsations from the Sun's surface. Are we not observing distant consequences of helioseismic pulsations on Earth?

Closing this discussion, we touch on the question of the ponderomotive force of ULF waves acting on the magnetospheric plasma [11]. The plasma consists of electrons, protons, helium ions, and a small fraction of oxygen ions of atmospheric origin. Propagating down along a geomagnetic field line, a sporadic wave packet of DSs of a falling tone stays for an extended time interval in the conditions of gyroresonance, with oxygen ions moving upward under the action of the ponderomotive force. This may lead to a kind of 'fountaining' of oxygen ions.

Sufficiently powerful pearl series can noticeably affect the distribution of plasma in the magnetosphere. In this case, the ponderomotive force of an ion-cyclotron wave may 'rake' the plasma to the minima of the geomagnetic field. At relatively small distances from Earth, a dipole field approximation can be applied, implying that the minima are located in the plane of the geomagnetic equator. Figure 15 shows the distribution of plasma density ρ along geomagnetic field lines as a function of the wave amplitude E [11, 103, 104]. Here, $X = \sin\varphi$, φ is the geomagnetic latitude, and $Y = \rho/\rho_0$, ρ_0 is the plasma density at $\varphi = 0$. We see that, if the wave amplitude is higher than some critical value, the density maximum is formed at the peak of the field lines.

7. Conclusions

We close by proposing a summary. Our general conclusion is such: the world of frequency modulated ULF waves, generously provided to us by nature, both surprises us and challenges our ability to understand all the diversity of modulation forms. It may seem that many things are already clear and do not cause doubt. They include a smooth daily variation in the frequencies of ionospheric resonators and a sharp jump in the carrier frequency of ion-cyclotron waves in the radiation belt on compression of the magnetosphere by an interplanetary shock wave. The theory on the excitation of pulsations of rising frequency in the evening sector by protons injected in the vicinity of the midnight meridian during magnetic storms also looks rather plausible in our opinion.

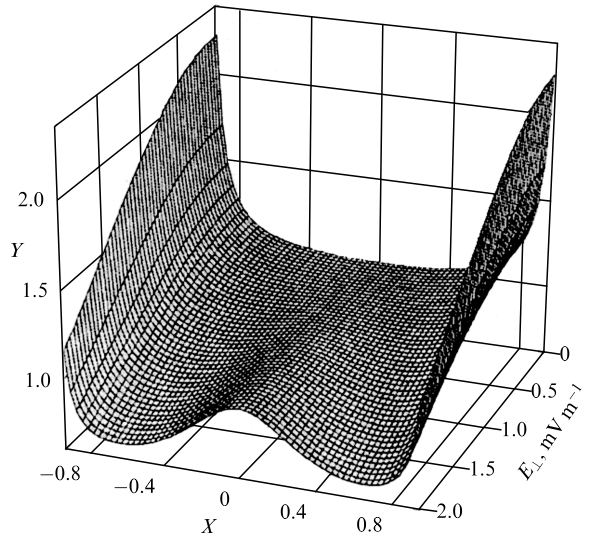

Figure 15. Redistribution of plasma density along geomagnetic field lines under the action of an ion-cyclotron wave (see the text).

However, the long history of key problems that defy solution is of concern. We list some of them.

We found that the impulse source of discrete signals penetrating into the polar caps is located upstream of the magnetospheric shock bow, but did not manage to understand the origin of the source. The theory of modulation of short ion-cyclotron waves in the interplanetary plasma by long Alfvén waves traveling from the Sun is supported only by terrestrial observations of serpentine emission. There is an urgent need to perform, but also a technical possibility of performing, direct observations in the interplanetary space using spacecraft. Success in this case would be the observation of serpentine emission outside the magnetosphere. The urgency of solving such a problem is that, judging by the available knowledge, the quasi-linear interaction of short-wave pulsations with solar wind protons essentially constrains the anisotropy in the proton velocity distribution.

The multitude of problems related to the excitation and propagation of pearl waves is the most difficult issue in our opinion. This variety of Pc1 waves was discovered by Sucksdorff and Harang in the mid-1930s. Since then, no other question has excited researchers of ULF waves as deeply as the question of the origin and properties of the pearls. Ideas have been proposed in abundance; the difficulty of the problem is both simulating and rewarding. Beginning in the 1960s, the pearls were and continue to be explored by geophysicists and space physicists using terrestrial and spacecraft-borne observational instruments, as well as sophisticated methods of theoretical analysis for linear and nonlinear wave processes. We mention an interesting question which was broadly discussed through the earlier stage of research: what serves as a trigger switching the radiation belt into the regime of self-excitation? Both endogenic and exogenic triggers have been studied, in particular, electromagnetic pulses penetrating into the magnetosphere from the interplanetary space as well as electromagnetic impulses of technogenic origin [105].

Two objective circumstances maintain the interest in the problem of pearl waves. The first lies in the fact that the self-excitation of waves in Earth's radiation belt leads to a natural limitation on the flux of energetic charged particles caught by

the geomagnetic trap. The second circumstance relies on a plausible assumption that a pearl-type wave phenomenon is not unique to Earth, but may occur on other planets possessing a magnetic field and, possibly, on more distant objects. In this respect, it is worthwhile to cite Ref. [106] which analyzes the so-called zebra structure in the spectrum of solar emission in the radio range, which remotely resembles the structure of the spectrum of a pearl necklace.

As a result of joint efforts, an internally consistent system of views has been elaborated, but it turns out that it does not correspond to reality. In our opinion, the key unsolved issues include the problem of how the discrete behavior is formulated and the problem of the specific dispersion of structural elements in the discrete sequence. A probable presence of an ion-cyclotron resonator located in the equatorial vicinity of the radiation belt makes the situation even more challenging. A question of the possible formation of a denser plasma in the vicinity of the equator through the ponderomotive action of waves on heavy ions of magnetospheric plasma creates new complications, yet arouses keen interest.

The research was carried out under the financial support of the Russian Foundation for Basic Research (grant nos 19-15-50043 and 19-05-00574), the Ministry for Education and Science of the Russian Federation (project RF KP19-270, program no. 0144-2014-00116 and subsidy no. 075-GZ/Ts3569/278), and Program No. 12 of the Presidium of the RAS. The observational data used in this study were obtained partly by the use of the equipment of the Angara Center of Joint Use (http://ckp-rf.ru/ckp/3056/). The authors are deeply indebted to B V Dovbnya, O D Zotov, B I Klain, T N Polyushkina, and F Z Feigin for their numerous fruitful discussions.

References

1. Belenkaya E S *Phys. Usp.* **52** 765 (2009); *Usp. Fiz. Nauk* **179** 809 (2009)
2. Troitskaya V A, Gul'elmi A V *Space Sci. Rev.* **7** 689 (1967)
3. Guglielmi A V, Pokhotelov O A *Geoelectromagnetic Waves* (Bristol: Institute of Physics Publ., 1996)
4. Guglielmi A V, Troitskaya V A *Geomagnitnye Pul'satsii i Diagnostika Magnitosfery* (Geomagnetic Pulsations and Diagnostics of the Magnetosphere) (Moscow: Nauka, 1973)
5. Mandel'shtam L I *Lektsii po Teorii Kolebanii* (Lectures on the Theory of Oscillations) (Moscow: Nauka, 1972)
6. Rytov S M "Modulirovannye kolebaniya i volny" ("Modulated oscillations and waves") *Tr. Fiz. Inst. Akad. Nauk SSSR* **2** (1) 41 (1940)
7. Gershman B N, Ugarov V A *Sov. Phys. Usp.* **3** 743 (1961); *Usp. Fiz. Nauk* **72** 235 (1960)
8. Likhter Ya I, Guglielmi A V, Erukhimov L M, Mikhailova G A *Volnovaya Diagnostika Prizemnoi Plazmy* (Wave Diagnostics of Near-Terrestrial Plasma) (Exec. Eds O A Molchanov, V N Oraevskii) (Moscow: Nauka, 1988)
9. Nishida A *Geomagnetic Diagnosis of the Magnetosphere* (New York: Springer-Verlag, 1978)
10. Kangas J, Guglielmi A, Pokhotelov O *Space Sci. Rev.* **83** 435 (1998)
11. Lundin R, Guglielmi A *Space Sci. Rev.* **127** 1 (2006)
12. Guglielmi A V *Phys. Usp.* **50** 1197 (2007); *Usp. Fiz. Nauk* **177** 1257 (2007)
13. Guglielmi A V, Potapov A S *Solar-Terr. Phys.* **5** (3) 87 (2019); *Solnechno-Zemn. Fiz.* **5** (3) 102 (2019)
14. Potapov A S et al. *J. Atmos. Solar-Terr. Phys.* **119** 91 (2014)
15. Guglielmi A V *Izv. Phys. Solid Earth* **42** 179 (2006); *Fiz. Zemli* (3) 3 (2006)
16. Guglielmi A V, Dovbnya B V *JETP Lett.* **18** 353 (1973); *Pis'ma Zh. Eksp. Teor. Fiz.* **18** 601 (1973)
17. Guglielmi A, Potapov A, Dovbnya B *Solar Phys.* **290** 3023 (2015)
18. Guglielmi A V, Potapov A S, Dovbnya B V *Solnechno-Zemn. Fiz.* **1** (2) 85 (2015)
19. Guglielmi A V, Potapov A S, arXiv:1808.05367
20. Parker E N *Interplanetary Dynamical Processes* (New York: Interscience Publ., 1963)
21. Guglielmi A V, Potapov A S, in *Proc. of the 2017 Progress in Electromagnetics Research Symp., Spring, PIERS, St. Petersburg, Russia, 22 – 25 May 2017* (Piscataway, NJ: IEEE, 2017) p. 1051
22. Hundhausen A J *Coronal Expansion and Solar Wind* (Physics and Chemistry in Space, Vol. 5) (Berlin: Springer-Verlag, 1972)
23. Guglielmi A V, Potapov A S *Geophys. Res.* **19** (4) 5 (2018); *Geofiz. Issled.* **19** (4) 5 (2018)
24. Kipper A Ya *Voprosy Kosmogonii* **8** 58 (1962)
25. Guglielmi A *Space Sci. Rev.* **16** 331 (1974)
26. Potapov A S *Issled. Geomagn. Aeron. Fiz. Solntsa* (34) 3 (1974)
27. Belcher J W, Davis L (Jr.) *J. Geophys. Res.* **76** 3534 (1971)
28. Bale S D et al. *Nature* **576** 237 (2019)
29. Guglielmi A V, Dovbnya B V *Astrophys. Space Sci.* **31** 11 (1974)
30. Fraser-Smith A C *Rev. Geophys.* **20** 497 (1982)
31. Asheim S "Serpentine emissions in the polar magnetic field", Report 83-38 (Oslo: Inst. of Physics, 1983)
32. Morris R J, Cole K D *Planet. Space Sci.* **35** 313 (1987)
33. Dovbnya B V et al. *Solar-Terr. Phys.* **3** (1) 73 (2017); *Solnechno-Zemn. Fiz.* **3** (1) 59 (2017)
34. Dovbnya B V, Potapov A S *Izv. Phys. Solid Earth* **54** 680 (2018); *Fiz. Zemli* (5) 19 (2018)
35. Leighton R B, Noyes R W, Simon G W *Astrophys. J.* **135** 474 (1962)
36. Vorontsov S V, Zharkov V N *Sov. Phys. Usp.* **24** 697 (1981); *Usp. Fiz. Nauk* **134** 675 (1981)
37. Potapov A S, Polyushkina T N, Pulyaev V A *Solnechno-Zemn. Fiz.* (20) 45 (2012)
38. Potapov A S, Polyushkina T N, Pulyaev V A *J. Atmos. Solar-Terr. Phys.* **102** 235 (2013)
39. Potapov A S, Polyushkina T N *Solnechno-Zemn. Fiz.* (15) 28 (2010)
40. Lessing L *Man of High Fidelity: Edwin Howard Armstrong, a Biography* (Philadelphia, PA: Lippincott, 1956)
41. Sucksdorff E *Terr. Magn. Atmos. Electricity* **41** 337 (1936)
42. Harang L *Terr. Magn. Atmos. Electricity* **37** 57 (1932)
43. Yanagihara K *J. Geophys. Res.* **68** 3383 (1963)
44. Cornwall J M *J. Geophys. Res.* **70** 61 (1965)
45. Tepley L *Radio Sci.* **69D** 1089 (1965)
46. Guglielmi A V *MGD-Volny v Okolozemnoi Plazme* (MHD Waves in Near-Terrestrial Plasma) (Moscow: Nauka, 1979)
47. Raita T, Kultima J *J. Atmos. Solar-Terr. Phys.* **69** 1600 (2007)
48. Ginzburg V L *The Propagation of Electromagnetic Waves in Plasmas* (Oxford: Pergamon Press, 1970); Translated from Russian: *Rasprostranenie Elektromagnitnykh Voln v Plazme* (Moscow: Nauka, 1967)
49. Lifshitz E M, Pitaevskii L P *Physical Kinetics* (Oxford: Pergamon Press, 1981); Translated from Russian: *Fizicheskaya Kinetika* (Moscow: Nauka, 1979)
50. Andronov A A, Fabrikant A L, in *Nelineinye Volny* (Nonlinear Waves) (Exec. Ed. A V Gaponov-Grekhov) (Moscow: Nauka, 1979) p. 68
51. Guglielmi A V *Geofiz. Issled.* **9** (3) 16 (2008)
52. Tverskoi B A *Dinamika Radiatsionnykh Poyasov Zemli* (Dynamics of Earth's Radiation Belts) (Moscow: Nauka, 1968)
53. Guglielmi A V, Potapov A S, Russell C T *JETP Lett.* **72** 298 (2000); *Pis'ma Zh. Eksp. Teor. Fiz.* **72** 432 (2000)
54. Kangas J, Fraser B, Potapov A *J. Atmos. Solar-Terr. Phys.* **69** 1599 (2007)
55. Demekhov A G *J. Atmos. Solar-Terr. Phys.* **69** 1609 (2007)
56. Mursula K *J. Atmos. Solar-Terr. Phys.* **69** 1623 (2007)
57. Zolotukhina N, Cao J *J. Atmos. Solar-Terr. Phys.* **69** 1668 (2007)
58. Kurazhkovskaya N A, Klain B I, Dovbnya B V *J. Atmos. Solar-Terr. Phys.* **69** 1680 (2007)
59. Yahnin A G, Yahnina T A *J. Atmos. Solar-Terr. Phys.* **69** 1690 (2007)
60. Paulson K W et al. *Geophys. Res. Lett.* **41** 1823 (2014)
61. Paulson K W et al. *J. Geophys. Res. Space Phys.* **122** 105 (2017)
62. Klimushkin D Yu, Mager P N, Marilovtseva O S *J. Atmos. Solar-Terr. Phys.* **72** 1327 (2010)
63. Mikhailova O S *J. Atmos. Solar-Terr. Phys.* **108** 10 (2014)

64. Nekrasov A K, Feygin F Z *Izv. Phys. Solid Earth* **54** 741 (2018); *Fiz. Zemli* (5) 81 (2018)
65. Feigin F Z, Yakimenko V L *Geomagn. Aeron.* **9** 700 (1969)
66. Feigin F Z, Yakimenko V L *Geomagn. Aeron.* **10** 558 (1970)
67. Feygin F Z, Kurchashov Yu P *J. Geomagn. Geoelectricity* **26** 539 (1975)
68. Guglielmi A, Kangas J, Potapov A *J. Geophys. Res.* **106** 25847 (2001)
69. Guglielmi A, Kangas J *J. Atmos. Solar-Terr. Phys.* **69** 1635 (2007)
70. Guglielmi A V, Potapov A S *Kosm. Issled.* **50** 283 (2012)
71. Landau L D, Lifshitz E M *Mechanics* (Oxford: Pergamon Press, 1976); Translated from Russian: *Mekhanika* (Moscow: Nauka, 1988)
72. Gul'el'mi A V *JETP Lett.* **13** 57 (1971); *Pis'ma Zh. Eksp. Teor. Fiz.* **13** 85 (1971)
73. Bespalov P A, Trakhtengerts V Yu *Al'venovskie Mazery* (Alfvén Masers) (Gor'kii: IPF AN SSSR, 1986)
74. Tagirov V R, Trakhtengerts V Yu, Chernous S A *Geomagn. Aeron.* **26** 600 (1986)
75. Trakhtengerts V Yu, Tagirov V R, Chernous S A *Geomagn. Aeron.* **26** 99 (1986)
76. Trakhtengerts V Yu, Demekhov A G *Priroda* (4) 25 (2002)
77. Trakhtengerts V Y, Rycroft M J *Whistler and Alfvén Mode Cyclotron Masers in Space* (Cambridge: Cambridge Univ. Press, 2008); Translated into Russian: *Svistovye i Al'fvenovskie Mazery v Kosmose* (Moscow: Fizmatlit, 2011)
78. Vainshtein L A *Sov. Phys. Usp.* **19** 189 (1976); *Usp. Fiz. Nauk* **118** 339 (1976)
79. Kravtsov Yu A, Orlov Yu I *Geometrical Optics of Inhomogeneous Media* (Berlin: Springer-Verlag, 1990); Translated from Russian: *Geometricheskaya Optika Neodnorodnykh Sred* (Moscow: Nauka, 1980)
80. Storey L R O *Philos. Trans. R. Soc.* **246** 113 (1953)
81. Carpenter D L *J. Geophys. Res.* **68** 1675 (1963)
82. Potapov A S *Geomagn. Aeron.* **13** 377 (1973)
83. Guglielmi A V, Klain B I, Potapov A S *Solar-Terr. Phys.* **3** (4) 26 (2017); *Solnechno-Zemn. Fiz.* **3** (4) 27 (2017)
84. Guglielmi A V, Potapov A S, Dovbnya B V *Geofiz. Issled.* **20** (2) 19 (2019)
85. Russell C T, Hoppe M M *Space Sci. Rev.* **34** 155 (1983)
86. Troitskaya V A, Mel'nikova M V "Yavlenie vozbuzhdeniya kvaziperiodicheskikh kolebanii magnitnogo polya Zemli narastayushchei chastoty" ("State catalog of discoveries of USSR. The phenomenon of excitation of quasi-periodic pulsations in Earth's magnetic field with raising frequency"), State Register of Discoveries of the USSR. Diploma No. 179. Priority from 4 July 1959
87. Troitskaya V A, Mel'nikova M V *Dokl. Akad. Nauk SSSR* **128** 917 (1959)
88. Troitskaya V A *J. Geophys. Res.* **66** 5 (1961)
89. Gendrin R et al. *Planet. Space Sci.* **15**1239 (1967)
90. Troitskaya V A, Shchepetnov R V, Guglielmi A V *Geomagn. Aeron.* **8** 794 (1968)
91. Mal'tseva N F, Guglielmi A V, Vinogradova V N *Geomagn. Aeron.* **10** 939 (1970)
92. Potapov A et al., in *Trigger Effects in Geosystems. The 5th Intern. Conf., Sadovsky Institute of Geospheres Dynamics of Russian Academy of Sciences* (Springer Proc. in Earth and Environmental Sciences, Eds G Kocharyan, A Lyakhov) (Cham: Springer, 2019) p. 579
93. Zolotukhina N A "Vozbuzhdenie geomagnitnykh pul'satsii v rezul'tate inzhektsii i nestatsionarnogo dreifa energichnykh chastits" ("Excitation of geomagnetic pulsations as a result of injection and nonstationary drift of energetic particles"), Ph.D. Thesis (Phys.-Math.) (Moscow: Institute of Physics of the Earth, USSR Academy of Sciences, 1979)
94. Zolotukhina N, Cao J *J. Atmos. Solar-Terr. Phys.* **69** 1668 (2007)
95. Guglielmi A V, Potapov A S *Solar-Terr. Phys.* **3** (3) 82 (2017); *Solnechno-Zemn. Fiz.* **3** (3) 95 (2017)
96. Burton R K, McPherron R L, Russell C T *J. Geophys. Res.* **80** 4204 (1975)
97. Potapov A S et al. *Solar-Terr. Phys.* **2** (4) 16 (2016); *Solnechno-Zemn. Fiz.* **2** (4) 13 (2016)
98. Feygin F Z, Yakimenko V L *Ann. Geophys.* **27** 49 (1971)
99. Gendrin R et al. *Planet. Space Sci.* **19** 165 (1971)
100. Guglielmi A, Pokhotelov O *Space Sci. Rev.* **65** 5 (1993)
101. Potapov A S, Polyushkina T N *IEEE Trans. Geosci. Remote Sensing* **58** 5058 (2020)
102. Leonovich A S, Mazur V A *Lineinaya Teoriya MGD-Kolebanii Magnitosfery* (Linear Theory of MHD-Oscillations of the Magnetosphere) (Moscow: Fizmatlit, 2016)
103. Guglielmi A V *Fiz. Zemli* (7) 35 (1992)
104. Guglielmi A V, Feigin F Z *Fiz. Zemli* (5) 53 (2018)
105. Guglielmi A V, Zotov O D *Izv. Phys. Solid Earth* **48** 486 (2012); *Fiz. Zemli* (6) 23 (2012)
106. Zlotnik E Ya *Solnechno-Zemn. Fiz.* **16** 49 (2010)